

*nduction motor, wavelet transformation,  
backlash zone, neural networks.*

*Marcin TOMCZYK*<sup>[0000-0002-5383-7168]\*</sup>,  
*Anna PLICHTA*<sup>[0000-0001-6503-308X]\*\*</sup>, *Mariusz MIKULSKI*<sup>\*\*\*</sup>

## **APPLICATION OF WAVELET – NEURAL METHOD TO DETECT BACKLASH ZONE IN ELECTROMECHANICAL SYSTEMS GENERATING NOISES**

### **Abstract**

*This paper presents a method of identifying the width of backlash zone in an electromechanical system generating noises. The system load is a series of rectangular pulses of constant amplitude, generated at equal intervals. The need for identification of the backlash zone is associated with a gradual increase of its width during the drive operation. The study uses wavelet analysis of signals and analysis of neural network weights obtained from the processing without supervised learning. The time-frequency signal representations of accelerations of the mechanical load components were investigated.*

---

\* Cracow Univeristy of Technology, Faculty of Electrical and Computer Engineering, Warszawska 24, 31-155 Kraków, Poland, marcin.tomczyk@pk.edu.pl

\*\* Cracow Univeristy of Technology, Faculty of Computer Science and Telecommunications, Chair of Computer Science, Warszawska 24, 31-155 Kraków, Poland, aplichta@pk.edu.pl

\*\*\* State Higher Vocational School in Nowy Sącz, Institute of Engineering, Zamenhofa 1a, 33-300 Nowy Sącz, Poland, mmikulsk1@poczta.onet.pl

## 1. INTRODUCTION

The diagnostics of electromechanical processes deals with the recognition of undesired changes of their states. The states are presented in the form of a sequence of intentional actions conducted in the assumed time by a specific set of machines and devices at a determined amount of available resources. Faults and other destructive events resulting from the wear and tear as well as increased exploitation time can be reasons for changes in these states. If such a change of state exceeds specific value it should be detected by a diagnostic system, recognized as fault, and identified as quickly as possible, in its early phase of formation (Korbicz, Kościelny & Kowalczyk, 2002).

Some information carried by signals appearing in electromechanical systems are essential for diagnostic reasoning, and particular attention should be paid to their extraction and application (Zhang, Zhu, Yang, Yao & Lu, 2007).

Measuring signals generated by sensors or converters using the measuring path are subjected to analysis. However, they often contain irrelevant content, i.e. trends or fast-changing components whose character resembles noise. The attempts to limit such unnecessary characteristics and using digital-to-analogue converters to guarantee appropriate value of signal-to-noise relation can result in side effects having negative impact on the analysis, e.g. frequency masking or stroboscopic effect. Therefore, sampling frequency must be appropriate to the components of the signal that contain relevant information (Zhang, Zhu, Yang, Yao & Lu, 2007).

In mechanical systems containing backlash zones, non-linear elastic-absorbing elements or faulted bearings, diagnostic signals pertaining to time and frequency can be generated using transformation methods that enable simultaneous testing of the spectral properties in both of these fields (Duda, 2007).

One of the increasingly popular and applied methods of time-frequency analysis is wavelet transformation based on multistage signal decomposition at changeable resolution (Duda, 2007; Zajac, 2009).

In contrast with Fourier analysis in which analysed functions are expressed by means of polynomials derived from harmonic functions, wavelet transformation describes them using special functions — wavelets derived from a dedicated function called mother wavelet. The created wavelet functions are subjected to repeated transformations. The set of base functions of transformation obtained in this way has a number important scalable properties related to the time and frequency; one can analyze the relationships between the particular function and its transformation coefficients (Doniec, 2010).

Owing to the recent progress in signal processing technology, many diagnostic methods have been presented that concern engine diagnostics by means of wavelet analysis. These are, for instance:

- discussion on the usefulness of wavelet analysis for the initial processing of diagnostic signals to train and test neural damage detectors of induction motors (Kowalski, 2003),

- detection of microcracks on the surface of bearing race (Zajac, 2009), on its rolling element (Chebil, Noel, Mesbah & Derihe, 2009), as well as in the bearing-connecting elements (Aktas & Turkmenoglu, 2010),
- analysis of electro-energetic signals by means of the high-resolution methods of spectrum analysis (Łobos, Leonowicz, Rezmer & Schegner, 2006),
- detection of rotor crack in induction cage motor by means of the frequency analysis using MCSA analysis as well as continuous wavelet transformation (Granda, Aguilar, Arcos-Aviles & Sotomayor, 2017).

Recently, more and more studies focus on the application of neural networks like, e.g.:

- using of single neural network to detect faults at the various stages of work of nuclear power plant (Wysogład, 2003),
- detection of faults in chemical plants by means of dynamic networks (Fuente & Saludes, 2000),
- solving problems pertaining to modelling and classification in the object and system diagnostic processes using GMDH networks (*Group Methods and Data Handling*) (Duch, Korbicz, Rutkowski & Tadeusiewicz, 2000). This study contains a lot of neural architectures with dynamic properties characterized by their excellent efficiency during modelling of diagnosed processes.
- identification of mechanical parameters in three-phase induction cage motor by means of model of neural network using gradient decrease method (Balara, Timko, Žilkova & Lešo, 2017).

## 2. METHODOLOGY AND ANALYSIS OF THE FAULT IDENTIFICATION DIAGNOSTIC ALGORITHM

Simulation tests were conducted for the nominal conditions of the induction motor whose model was located in a stationary coordinate system related to the stator (model  $\alpha, \beta, 0$ ). The induction motor was loaded by a working machine similar in character to a dynamic mass-absorbing-elastic element.

Model of induction motor has been created in the MATLAB/Simulink environment. The following parameters of induction motor have been assumed in the conducted tests (parameters of the substitute scheme are expressed in relative units):  $r_S = 0.059$ ,  $r_w = 0.048$ ,  $x_S = 1.92$ ,  $x_R = 1.92$ ,  $x_M = 1.82$ ,  $w = x_S * x_w + x_m * x_m = 0.374$ ,  $T_m = 0.86$  [s].

Fig.1 presents a simplified diagram of connection of a working machine with the induction motor. The diagram includes backlash in the clutch connecting the induction motor drive with a working machine. It also includes the connection between the generator of normally distributed signals and generator of rectangular impulses and the dynamic mass-absorbing-elastic element and load moment.

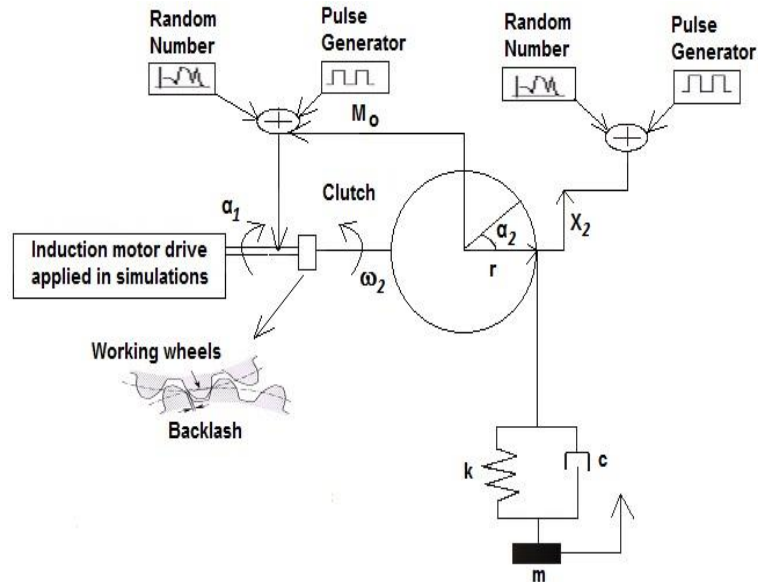


Fig.1. Diagram of a dynamic mass-absorbing-elastic element connected to the induction motor used in the simulation tests.

### 3. METHODOLOGY OF TESTS DEDICATED TO IDENTIFY CHANGES OF WIDTH OF BACKLASH ZONE IN THE ELECTROMECHANICAL SYSTEM GENERATING NOISES (FRICTION MODEL DESCRIBED USING OSTWALD-WAELE RELATIONSHIP)

Simulation tests of wavelet scalograms for coefficients of wavelet expansions of two physical quantities have been conducted: linear acceleration on the circuit of the drive wheel of motor's rotor  $a_1$  and linear acceleration of lifted mass of dynamic mass-absorbing-elastic element  $a_2$ . The results of simulation tests for each physical quantities were written in the matrix  $M_1$ .

Additionally, generator of rectangle impulses and generator of normally distributed signals were connected to the electromechanical system

Sampling time of normally distributed random numbers generator was equal to  $2 \cdot 10^{-4}$  [s]. Sampling time of impulses in generator of rectangle impulses was equal  $2 \cdot 10^{-3}$  [s]. For both generators variance has been assumed equal 0.05 and mean value equal 0.

Simulation tests have been executed in the following way.

For all measurements of faults (in four groups of tests) the same values were provided: the elasticity coefficient  $k = 100$  [N/m], radius  $r = 0.15$  [m], mass  $m = 10$  [kg] and surface area of absorber's cylinder  $S_1 = 0.00311565$  [m<sup>2</sup>]. In the next groups of tests the following values of consistency coefficient

(apparent viscosity) was assumed:  $\eta_k = 0.0125$  [Pa·s<sup>*n*<sub>1</sub></sup>],  $\eta_k = 0.025$  [Pa·s<sup>*n*<sub>1</sub></sup>],  $\eta_k = 0.0375$  [Pa·s<sup>*n*<sub>1</sub></sup>] and  $\eta_k = 0.05$  [Pa·s<sup>*n*<sub>1</sub></sup>]. During the measurements in each group of simulation tests the creep index  $n_1$  for a pseudo-plastic liquid was assumed amounting to: 0.89, 0.91, 0.93, 0.95 and 0.97. The values of the creep index  $n_1$  in the tests were written in matrix  $K_1$  in the ascending order.

In each test in which the value of the creep index  $n_1$  was changing, one conducted simulation tests, the width of backlash zone amounted to: 0.0025, 0.00375, 0.005, 0.0075, 0.009 and 0.01, in the above order.

In matrix  $K_2$ , widths of backlash zone applied in the conducted simulation tests were written in an ascending order.

In all the executed simulation tests, the principle was followed according to which the process of testing the electromechanical system dynamics within the backlash zone begins in the moment when the expression in the left part of the following inequality (1) is smaller than the expression in its right part:

$$|\alpha_1 - \alpha_2| < \frac{K_{2(i)}}{r}; \quad i = 1, 2..6 \quad (1)$$

where:  $r$  – radius of the drive wheel of a working machine [m],

$K_2$  – value that has been taken sequentially from the matrix and corresponding to the assumed width of backlash zone in mechanical connection,

$i$  – an index number of matrix's column  $K_2$ .

Values of angles have been calculated according to the following formulas:

$$\alpha_1 = \int \omega_1 \cdot dt \quad (2)$$

$$\alpha_2 = \int \omega_2 \cdot dt \quad (3)$$

After meeting the condition determined by inequality described by the formula (1) load torque of the dynamic mass-absorbing-elastic element is zeroed.

Matrix  $M_1$  contained 2048 sequentially chosen samples recorded after the occurrence of backlash zone in the tested model. This experiment has been carried out for every measurement of both tested physical quantities. Fig. 2 presents the example of collecting samples in backlash zone against the linear acceleration of the mass of the dynamic mass-absorbing-elastic element.

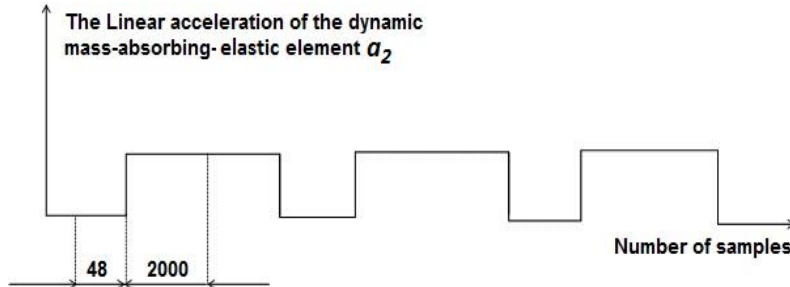


**Fig. 2. Testing of dynamics in the backlash zone by means of the choice of time range**

Removal of noises from all the variables placed in matrix  $M_1$  has been executed by means of removal of relevant details of a given wavelet for the particular variable. Subsequently, the registered samples have been written in matrix  $M_2$ .

A signal obtained after the removal of details has been written sequentially for the appropriate value of the creep index  $n_1$  in matrix  $M_2$  whose dimension amounted to  $6 \times 2048$ .

The wavelet type and order have been selected so that the shape of the basic wavelet would be approximately adequate to the character of the transient course of the physical quantity obtained in the test for the smallest backlash value.

After conducting the tests for the respective variables, the following wavelets were chosen:

- a)  $a_1$  – wavelet function symlet of the order 5,
- b)  $a_2$  – wavelet function symlet of the order 5.

On the basis of calculations conducted for the generator of normally distributed random numbers, decomposition (number of detail) level has been determined amounting to 2 whereas for the generator of rectangle impulses decomposition level (number of detail) was equal to 6.

After the tests of hard and soft elimination for the analyzing wave, the noises placed in matrix  $M_1$  were removed, which consisted, e.g. in the removal of details whose frequencies were similar to the frequencies of the disturbing impulses.

By means of the calculated decomposition levels for both generators used in the simulation tests and as a result of observation of frequencies of disrupting impulses, the following numbers of details for variables  $a_1$  and  $a_2$  were deleted: 1, 2, 3, 4, 5, 6.

#### 4. DESCRIPTION OF PROCESSING OF TWO-LAYER NEURAL NETWORK OF TYPE *COUNTER-PROPAGATION*

In the conducted simulation tests, two-layer neural network was learnt without the supervision for the values of matrix  $M_2$ .

The first layer of this network is named Kohonen's layer and represents a set of exemplary pairs of input signals of neural network  $X_1$  and values of weights  $W_1$ . In the second layer of this network, named Grossberg's layer,  $X_2$  values represent input signals while  $W_2$  values represent the given set of the exemplary weights.

The input signals of neural network in the first layer represent Kohonen's layer were calculated in matrix  $X_1$  according to the formula:

$$X_{1(j)} = M_{2(p)(j)}; j = 1, 2 \dots 2048; p \in \langle 1, 6 \rangle \quad (9)$$

where:  $M_{2(p)(j)}$  – values of matrix for the tested width of backlash zone and registered for the applied values of the creep index  $n_1$ ,  
 $p$  – number of column in  $K_1$  matrix.

According to the assumptions typical of *Counter-Propagation* networks, values of input signals must be normalised to fulfill the condition (Tadeusiewicz, 1993):

$$X_1^T * X_1 = 1 \quad (11)$$

Normalization of input signals  $X_1$  is conducted according to the formula:

$$X_{1(i)} = \frac{X_{1(i)}}{\sum_{j=1}^{2048} (X_{1(j)})^2}; \quad i = 1, 2 \dots 2048 \quad (12)$$

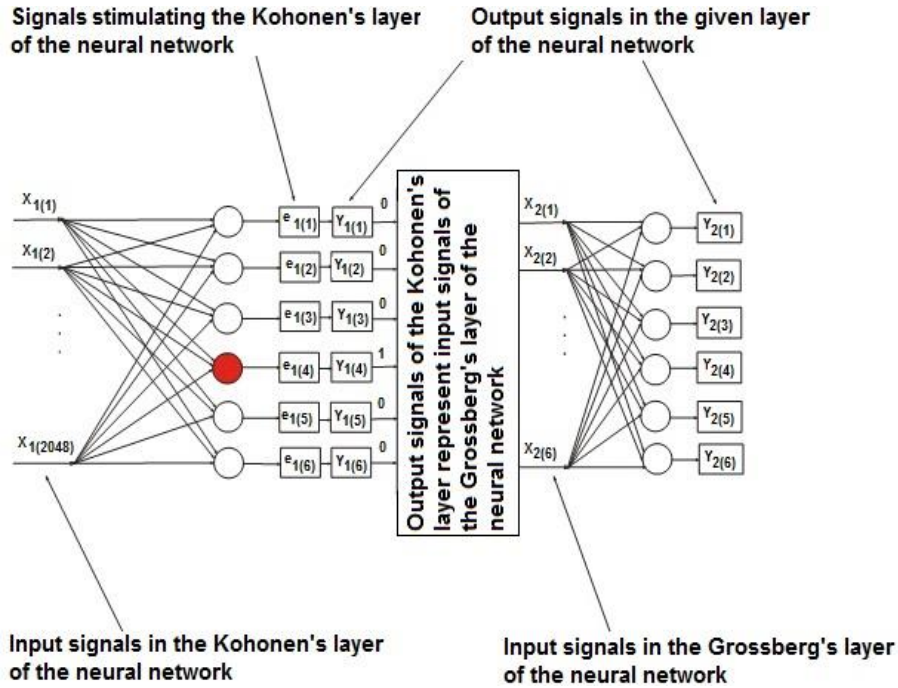


**Fig. 3. Diagram of the used neural network dedicated to identification of width of backlash zone in the electromechanical system generating noises with viscous and fluid friction described by means of Ostwald–de Waele power equation (the circles represent neurons in neural network; the red neuron in the Kohonen's layer indicates a random 'winner neuron')**

The aim of normalization of input signals carried out in the simulation tests was to ensure the appropriate adaptation of values of weights  $W_1$  during the processing of neural network.

The selection of number of epochs in the discussed model of two-layer neural network was determined experimentally on the basis of observation of the obtained values of  $W_2$  weights.

The initial values of weights in the first layer  $W_1$  were determined according to the formula:

$$W_{1(i,j)} = M_{3(i)}; i = 1,2...6; j = 1,2...2048 \quad (13)$$

where:  $M_3$  – calculated arithmetic means of matrix  $M_2$  rows for the value of the creep index  $n_1$  amounting to 0.89 for the group of simulation tests in which the consistency coefficient  $\eta_k$  was equal to 0.025.

Arithmetic means of matrix  $M_2$  rows were calculated in matrix  $M_3$  according to the formula:

$$M_{3(i)} = \frac{\sum_{j=1}^{2048} M_{2(p)(i,j)}}{2048}; \quad i = 1, 2 \dots 6; p = 1 \quad (14)$$

where:  $M_2$  – values of matrix recorded in the simulation tests at the value of the creep index  $n_1$  equal to 0.89 for the group of tests in which the consistency coefficient  $\eta_k$  was equal to 0.025;  $p = 1$  stands for the number of column in the matrix  $K_1$ .

Multiplication of input signals  $X_1$  by values of weights  $W_1$  of the particular neurons of the first layer of neural network results in the calculation of signals  $E_1$  according to the formula:

$$E_{1(i)} = \sum_{j=1}^{2048} X_{1(j)} * W_{1(i,j)}; \quad i = 1, 2 \dots 6 \quad (15)$$

Signals  $E_1$  represent total stimulations of all neurons in the first layer from which the so-called “winner neuron” is selected having maximum value of the stimulation determined on basis of the following formula:

$$E_{1(t)} = \max(E_{1(i)}); \quad i = 1, 2 \dots 6; t \in \langle 1, 6 \rangle \quad (16)$$

Therefore, only for the victorious neuron output signal  $Y_1$  has the value equal to 1 according to the equation:

$$Y_{1(i)} = \begin{cases} 1; & i = t \\ 0; & i \neq t \end{cases} \quad i = 1, 2 \dots 6; t \in \langle 1, 6 \rangle \quad (17)$$

The correction of weights is a result of product of difference between the input value  $X_1$  and weight associated with:

- input value  $W_1$ ,
- experimentally selected learning coefficient of neural network  $l_1$  whose the range varies from 0 to 1.

The correction of weights for the “winner neuron” in the first layer of neural network  $W_1$  was calculated by means of the well-known WTA (*Winner Takes All*) rule according to the formula (Osowski, 1996):

$$W_{1(t,j)} = W_{1(t,j)} + l_1 \cdot (X_{1(t,j)} - W_{1(t,j)}); \quad j = 1, 2 \dots 2048; t \in \langle 1, 6 \rangle \quad (18)$$

Input signals of the second layer of neural network representing Grossberg's layer were calculated in matrix  $X_2$  according to the formula:

$$X_{2(j)} = Y_{1(i)}; i = 1, 2 \dots 6; j = 1, 2 \dots 6; \quad (19)$$

The applied initial values of matrix weights of the second layer in matrix  $W_2$  were the same for the particular neurons placed in this layer and determined on the basis of the formula:

$$W_{2(i,j)} = m_1; i = 1, 2 \dots 6; j = 1, 2 \dots 6; \quad (20)$$

where:  $m_1$  – arithmetic mean of matrix  $M_3$  determined on the basis of the formula (14).

The arithmetic mean  $m_1$  was calculated according to the formula:

$$m_1 = \frac{\sum_{i=1}^6 M_{3(i)}}{6} \quad (21)$$

The advantage of processing of this neural network is the possibility of setting relatively small number of epochs and therefore obtaining the values of weights  $W_2$  in the second layer appropriate for diagnostic purposes.

The output signals of the second layer of neural network  $Y_2$  were calculated according to the formula:

$$Y_{2(i)} = \sum_{j=1}^6 X_{2(j)} * W_{2(i,j)}; \quad i = 1, 2 \dots 6 \quad (22)$$

Correction of weights results from the product of difference between:

- output value  $Y_2$ ,
- the set value  $Z_1$  associated with:  $Y_2$ , input value  $X_2$ , and experimentally selected learning coefficient of neural network  $l_2$  whose range varies from 0 to 1.

Correction weights in this layer of neural network  $W_2$  was calculated on the basis of well-known “outstar” rule (Osowski, 1996) according to the formula:

$$W_{2(i,j)} = W_{2(i,j)} + l_2 \cdot (Y_{2(i)} - Z_{1(i)}) \cdot X_{2(j)}; i = 1, 2 \dots 6; j = 1, 2 \dots 6 \quad (23)$$

where:  $Z_1$  – matrix of set values of neural network.

The applied set values  $Z_1$  were the same for all the neurons in Grossberg's layer and calculated according to the formula:

$$Z_{1(i)} = m_2; i = 1, 2 \dots 6 \quad (24)$$

where:  $m_2$  – the arithmetic mean of values of matrix  $M_2$  for the tested width of backlash zone at the given value of creep index  $n_1$ .

The arithmetic mean  $m_2$  was calculated according to the formula:

$$m_2 = \frac{\sum_{j=1}^{2048} M_{2(p)(j)}}{2048}; \quad j = 1, 2 \dots 2048; p \in \langle 1, 6 \rangle \quad (25)$$

To identify the width of backlash zone for all the tested physical quantities one had to create pattern vectors  $W_5$  as well as tested vectors  $W_6$ . These vectors were registered during the simulation tests for the assumed value of creep index  $n_1$ . Pattern vectors  $W_5$  were created for the group of simulation tests conducted at the consistency coefficient  $\eta_k = 0.025$ .

To determine both pattern vectors and tested vector, maximum value  $T_2$  was determined on the basis of all the weights placed in the Grossberg's layer  $W_2$  subjected to the following formula:

$$T_2 = \max (W_{2(i,j)}); \quad i=1, 2 \dots 6; j=1, 2 \dots 6 \quad (26)$$

The decision to select maximum value among all weights  $W_2$  instead of minimum weight, necessary in determining pattern vectors and tested vector, proved to be a correct strategy.

On the basis of maximum value  $T_2$  matrix  $W_3$  was determined according to the formula:

$$W_{3(j)} = W_{2(d,j)}; T_2 \in W_{2(d,j)}; d \in \langle 1, 6 \rangle; j = 1, 2 \dots 6 \quad (27)$$

During the simulation tests dedicated to identify width of backlash zone at the changing value of consistency coefficient  $\eta_k$ , different "winner neurons" in the Kohonen's layer were selected. This fact resulted from the use of different values of input signals  $X_1$  for this same value of the creep index  $n_1$ , which caused disruption of order of the obtained values weights  $W_2$  in the Grossberg's layer.

Sorting the values of matrix  $W_3$  instead of assuming different numbers of input signals  $X_1$  is a factor responsible for a significant versatility of the presented diagnostic method due to the possibility of using this procedure in the case of more physical quantities to test.

In the presented diagnostic method matrix  $W_3$  was sorted in the descending order. After sorting, the value of this matrix was written in matrix  $W_4$  according to the following formula:

$$W_4 = [W_{3(1)} \geq W_{3(2)} \geq W_{3(3)} \geq \dots \geq W_{3(6)}] \quad (28)$$

Pattern vectors  $W_5$  as well as tested vector  $W_6$ , used in identification of width of backlash zone, were determined, respectively, according to the formula:

$$W_{5(i,j)} = W_{4(i,j)}; \quad i = 1,2\dots6; j = 1,2\dots6 \quad (29)$$

$$W_{6(j)} = W_{4(j)}; \quad j = 1,2\dots6 \quad (30)$$

Identification of the assumed width of backlash zone at the assumed value of the creep index  $n_1$  is possible owing to the calculation of values of matrix  $B$  according to the formula:

$$B_{(i)} = \sum_{j=1}^6 |W_{6(j)} - W_{5(i,j)}|; \quad i = 1,2\dots6 \quad (31)$$

Determination of minimal value of matrix  $B$  causes determination of index  $nr_1$  according to the following formula:

$$B_{(nr_1)} = \min(B_{(d)}); \quad d = 1,2\dots6; nr_1 \in \langle 1,6 \rangle \quad (32)$$

Calculations concerning the value of index  $nr_1$  are necessary for the correct identification of width of backlash zone determined on the basis of the particular number of column  $K_2$  referring to this index according to the formula:

$$i = nr_1 \quad (33)$$

where:  $i$  – number of column in matrix  $K_2$ .

## 5. RESULTS OF SIMULATION FOR DIAGNOSTIC ALGORITHM DEDICATED TO IDENTIFICATION OF WIDTH OF BACKLASH ZONE IN ELECTROMECHANICAL SYSTEM GENERATING NOISES

In the tables below, the column labeled *Test parameters* contains widths of backlash zone identified in the tests. However, the column *Results* comprises the bolded final results of calculations of values of matrix  $B$ .

**Tab. 1. Selected values of matrix  $B$  for linear acceleration of the induction motor  $a_1$  in electro-mechanical system containing friction described by means of Ostwald – de Waele power equation**

Test parameters	Results	Test parameters	Results
backlash zone = 0.009, consistency coefficient $\eta_k = 0.0125$ , creep index $n_1 = 0.91$ , epochs = 30, learning coefficient of neural network $l_1 = 0.1$ , learning coefficient of neural network $l_2 = 0.09$	1.5895 0.9248 0.2620 0.4710 <b>0.0025</b> 0.8902	backlash zone = 0.009, consistency coefficient $\eta_k = 0.0125$ , creep index $n_1 = 0.91$ , epochs = 30, learning coefficient of neural network $l_1 = 0.1$ , learning coefficient of neural network $l_2 = 0.01$	0.0859 0.0500 0.0142 0.0255 <b>0.0001</b> 0.0481
backlash zone = 0.0025, consistency coefficient $\eta_k = 0.05$ , creep index $n_1 = 0.95$ , epochs = 30, learning coefficient of neural network $l_1 = 0.1$ , learning coefficient of neural network $l_2 = 0.09$	<b>0.2949</b> 0.9600 1.6225 2.3551 1.8860 0.9922	backlash zone = 0.0025, consistency coefficient $\eta_k = 0.05$ , creep index $n_1 = 0.95$ , epochs = 30, learning coefficient of neural network $l_1 = 0.9$ , learning coefficient of neural network $l_2 = 0.01$	<b>0.0165</b> 0.0538 0.0910 0.1321 0.1058 0.0557
backlash zone = 0.005, consistency coefficient $\eta_k = 0.0375$ , creep index $n_1 = 0.97$ , epochs = 20, learning coefficient of neural network $l_1 = 0.1$ , learning coefficient of neural network $l_2 = 0.09$	0.5442 0.2718 <b>0.0003</b> 0.2998 0.1076 0.2585	backlash zone = 0.005, consistency coefficient $\eta_k = 0.0375$ , creep index $n_1 = 0.97$ , epochs = 40, learning coefficient of neural network $l_1 = 0.1$ , learning coefficient of neural network $l_2 = 0.09$	3.18481 0.5904 <b>0.0019</b> 1.7545 0.6297 1.5130

**Tab. 2. Selected calculated values of matrix  $B$  for linear acceleration of a mass  $a_2$  in electro-mechanical system containing friction described by means of Ostwald-de Waele power equation**

Test parameters	Results	Test parameters	Results
backlash zone = 0.009, consistency coefficient $\eta_k = 0.0125$ , creep index $n_1 = 0.93$ , number of epochs = 30, learning coefficient of neural network $l_1 = 0.1$ , learning coefficient of neural network $l_2 = 0.09$	0.6245 0.4992 0.3698 0.1376 <b>0.0002</b> 0.0868	backlash zone = 0.009, consistency coefficient $\eta_k = 0.0125$ , creep index $n_1 = 0.93$ , number of epochs = 30, learning coefficient of neural network $l_1 = 0.1$ , learning coefficient of neural network $l_2 = 0.01$	0.0517 0.0413 0.0306 0.0114 <b><math>1.5565 \cdot 10^{-5}</math></b> 0.0072
backlash zone = 0.00375, consistency coefficient $\eta_k = 0.05$ , creep index $n_1 = 0.89$ , number of epochs = 30, learning coefficient of neural network $l_1 = 0.1$ , learning coefficient of neural network $l_2 = 0.09$	0.1256 <b>0.0003</b> 0.1292 0.3613 0.4988 0.5857	backlash zone = 0.00375, consistency coefficient $\eta_k = 0.05$ , creep index $n_1 = 0.89$ , number of epochs = 30, learning coefficient of neural network $l_1 = 0.9$ , learning coefficient of neural network $l_2 = 0.01$	0.2931 <b>0.0006</b> 0.3016 0.8434 1.1643 1.3672
backlash zone = 0.0025, consistency coefficient $\eta_k = 0.0375$ , creep index $n_1 = 0.91$ , number of epochs = 20, learning coefficient of neural network $l_1 = 0.1$ , learning coefficient of neural network $l_2 = 0.09$	<b>0.0001</b> 0.0761 0.1550 0.2963 0.3800 0.4330	backlash zone = 0.0025, consistency coefficient $\eta_k = 0.0375$ , creep index $n_1 = 0.91$ , number of epochs = 40, learning coefficient of neural network $l_1 = 0.1$ , learning coefficient of neural network $l_2 = 0.09$	<b>0.0003</b> 0.1799 0.3663 0.7003 0.8980 1.0231

Bolded values of matrix  $B$  in the presented tables are correct results obtained finally in the process of identification of the fault number.

Pattern vectors  $W_5$  were registered in the simulation tests in which one applied the learning coefficient of Kohonen's layer  $l_1$ , the learning coefficient of Grossberg's layer  $l_2$ , and the number of epochs of processing of neural network consistent to the assumed values of these variables placed in the above presented tables.

For both tested physical quantities pattern vectors  $W_5$  were created in the group of simulation tests for which value of the assumed consistency coefficient  $\eta_k$  was 0.025.

In the conclusion, the number of epochs of processing of neural network was fixed to 30 because it ensured the greatest selection of values of elements of matrix  $B$  in comparison with the results of calculations for the number of epochs between 20 and 40.

On the basis of the presented results, one can notice that for both tested physical quantities, in the experiment consisting in linear acceleration of the induction motor  $a_1$  and also linear acceleration of mass  $a_2$ , values of matrix  $B$  gradually deteriorate for the learning coefficient of Kohonen's layer  $l_1$  decreasing in the range from 0.1 to 0.9 and for the learning coefficient of Grossberg's layer  $l_2$  increasing in the range from 0.09 to 0.01.

## 6. CONCLUSIONS

Using of time-frequency methods with multistage signal decomposition and also two-layer neural network processed without supervised learning was applied to monitor electromechanical system being in the backlash zone that included mass-absorbing-elastic load and where noises generated by means of generator of Gauss and generator of rectangle impulses (at the sampling frequency 50 kHz) brought disturbances to the received signals.

Distributions of coefficients of wavelet expansion of state variables that describe the tested physical quantities and the obtained values of weights of the second layer of the processed neural network – used for the linear acceleration on circuit of the drive wheel of motor  $A_1$  and linear acceleration  $A_2$  dynamic mass-absorbing element – enable obtaining of the correct results of identification of width of backlash zone. The simulation tests proved that the blur of spectrum, difficulties in obtaining small deviations from the state considered as correct and its nonlinear deformation may result from the inappropriate selection of the base wavelet.

It should be carefully chosen taking into account the character of the tested course on the basis of the:

- selection of the central frequency of signal associated with fault,
- frequency determined on the basis of sampling time of the generator of normally distributed random numbers,
- sampling time of generator of rectangle impulses.

The obtainment of better shapes of de-noised signals and consequent obtainment of correct final results of identification of width of backlash zone for the model of complex electromechanical system (usually described by nonlinear characteristics of elements) was possible owing to:

- the additional removal of some physical quantities of the tested electromechanical system apart from the calculated decomposition levels (details) of the assumed wavelet,
- determination of variance and mean value of random signals introduced by means of Gaussian generator and generator of rectangle impulses.

## REFERENCES

- Aktas, M., & Turkmenoglu, V. (2010). Wavelet-based switching faults detection in direct torque control induction motor drives. *Science, Measurement & Technology, IET*, 4(6), 303–310.
- Balara, D., Timko, J., Žilkova, J., & Lešo, D. (2017). Neural networks application for mechanical parameters identification of asynchronous motor. *Neural Network World*, 3, 259–270.
- Chebil, J., Noel, G., Mesbah, M., & Derihe, M. (2009). Wavelet Decomposition for the Detection and Diagnosis of Faults in Rolling Element Bearings. *Jordan Journal of Mechanical and Industrial Engineering*, 3(4), 260–267.
- Doniec, R. (2010). *Wykorzystanie metod sztucznej inteligencji do regulacji poziomu insuliny w organizmie człowieka* (doctoral dissertation). Politechnika Śląska, Gliwice.
- Duch, W., Korbicz, J., Rutkowski, L., & Tadeusiewicz, R. (2000). *Biocybernetyka i inżynieria biomedyczna 2000. Sieci neuronowe*. Tom 6. Warszawa: Akademicka Oficyna Wydawnicza EXIT.
- Duda, J. T. (2007). *Pozyskiwanie wzorców diagnostycznych w komputerowych analizach sprawności urządzeń, Diagnostyka procesów i systemów* (pp. 1–16). Warszawa: Akademicka Oficyna Wydawnicza EXIT.
- Fuente, M. J., & Saludes, S. (2000). Fault detection and isolation in a non-linear plant via neural networks. *IFAC Proceedings Volumes*, 33(11), 463–468.
- Granda, D., Aguilar, W. G., Arcos-Aviles, D., & Sotomayor, D., (2017). Broken bar diagnosis for squirrel cage induction motors using frequency analysis based on MCSA and continuous wavelet transform. *Mathematical and Computational Applications*, 22(2), 30. doi:10.3390/mca22020030
- Korbicz, J., Kościelny, J. M., & Kowalczyk, Z. (2002). *Diagnostyka procesów. Modele. Metody sztucznej inteligencji. Zastosowania*. Warszawa: WNT.
- Kowalski, Cz. (2003). Stan obecny i tendencje rozwojowe metod monitorowania i diagnostyki napędów z silnikami indukcyjnymi. *Wiadomości Elektrotechniczne*, 4, 160–164.
- Łobos, T., Leonowicz, Z., Rezmer, J., & Schegner, P. (2006). High resolution spectrum-estimation methods for signal analysis in power systems. *IEEE Trans. Instrum. Measur.*, 55(1), 219–225.
- Osowski, S. (1996). *Sieci neuronowe – w ujęciu algorytmicznym*. Warszawa: WNT.
- Tadeusiewicz, R. (1993). *Sieci neuronowe*. Warszawa: Akademicka Oficyna Wydawnicza.
- Wysogład, B. (2003). Metody diagnozowania łożysk tocznych z zastosowaniem transformacji falkowej. *Diagnostyka*, 29, 47–52.
- Zajęc, M. (2009). *Metody falkowe w monitoringu i diagnostyce układów elektromechanicznych*. Monografia 371. Kraków: Politechnika Krakowska.
- Zhang, J. W., Zhu, N., Yang, L., Yao, Q., & Lu, Q. (2007). A fault diagnosis approach for broken rotor bars based on EMD and envelope analysis. *Journal of China University Mining & Technology*, 17(2), 205–209.